

Text S1 The analysis of adsorption kinetic and isotherm of Pb(II) on biochar

Pseudo-first order (Eq.1), pseudo-second order (Eq.2), and Elovich (Eq.3) models were used to fit the data of adsorption kinetic, which are expressed as followed:

$$Q_t = Q_e(1 - e^{-k_1 t}) \quad (1)$$

$$Q_t = (Q_e^2 k_2 t) / (1 + Q_e k_2 t) \quad (2)$$

where Q_t (mg g^{-1}) and Q_e (mg g^{-1}) are the amounts of Pb(II) adsorbed at time t and at equilibrium, respectively, k_1 (h^{-1}) represents the rate constant of pseudo-first-order model, and k_2 is the rate constant of the pseudo second-order model ($\text{g mg}^{-1} \text{h}^{-1}$).

$$Q_t = a + b \ln(t) \quad (3)$$

where Q_t (mg g^{-1}) is the amounts of Pb(II) adsorbed at time t , a , and b are constants.

The Langmuir (Eq. 4) and Freundlich (Eq. 5) model were applied to simulate the adsorption isotherm data.

$$Q_e = K_L q_{\max} C_e / (1 + K_L C_e) \quad (4)$$

where Q_e (mg g^{-1}) and C_e (mg L^{-1}) are the adsorbed amount of Pb(II) by biochar and Pb(II) concentration at equilibrium solution, K_L (L mg^{-1}) is the Langmuir affinity constant, and q_{\max} (mg g^{-1}) is the theoretical maximum adsorption capacity as the monolayer surface is completely covered.

$$Q_e = K_F C_e^{1/n} \quad (5)$$

where K_F [$(\text{mg g}^{-1}) (\text{L mg}^{-1})^{1/n}$] and n are the constants related to adsorption capacity and intensity, respectively.

Table S1. The TG-DTG characteristic parameters of cotton stalk, LDPE and their mixture.

| | First Stage | | | | Second Stage | | | |
|------|----------------|----------------|------------------|------------------------------------|----------------|----------------|------------------|------------------------------------|
| | T _i | T _f | T _{max} | Residue at T _{max} (%) | T _i | T _f | T _{max} | Residue at T _{max} (%) |
| CS | 190.2 | 382.6 | 348.8 | 50.19 | - | - | - | - |
| LDPE | - | - | - | - | 390.5 | 503.9 | 474.6 | 35.06 |
| C3P1 | 189.9 | 382.1 | 347.2 | 64.06 | 433.7 | 505.3 | 476.8 | 34.60 |
| C2P1 | 189.5 | 382.4 | 345.7 | 67.97 | 431.5 | 505.0 | 479.8 | 34.35 |
| C1P1 | 189.3 | 381.8 | 344.3 | 76.27 | 425.9 | 504.5 | 480.5 | 34.59 |

Table S2. The maximum Pb(II) adsorption capacities of biochar co-pyrolyzed by cotton stalk and LDPE, other biomass.

| Adsorption Conditions | | Q _{max} (mg/g) | Ref. |
|----------------------------|--------------------------|-------------------------|---------------|
| Cotton stalk+LDPE | pH = 5.0, t = 24 h, 303K | 199.82 | in this study |
| Rice husk | pH = 5.0, t = 24 h, 298K | 2.40 | [1] |
| Pinewood | pH = 5.0, t = 24 h, 298K | 4.25 | |
| British broadleaf hardwood | pH = 5.0, t = 24 h, 293K | 47.66 | [2] |
| Corn stalk | pH = 5.5, t = 12h, 298K | 49.70 | [3] |
| Rice husk | - | 26.70 | [4] |
| Pine needle | pH = 5.0, t = 48 h, 308K | 40.43 | [5] |
| Saw dust | pH = 5.0, t = 24 h, 298K | 62.68 | [6] |

- [1] Z. Liu, F.-S. Zhang, Removal of lead from water using biochars prepared from hydrothermal liquefaction of biomass, *Journal of Hazardous Materials*, 167 (2009) 933-939.
- [2] Z. Shen, F. Jin, F. Wang, O. McMillan, A. Al-Tabbaa, Sorption of lead by Salisbury biochar produced from British broadleaf hardwood, *Bioresource Technology*, 193 (2015) 553-556.
- [3] L. Liu, Y. Huang, S. Zhang, Y. Gong, Y. Su, J. Cao, H. Hu, Adsorption characteristics and mechanism of Pb(II) by agricultural waste-derived biochars produced from a pilot-scale pyrolysis system, *Waste Management*, 100 (2019) 287-295.
- [4] J. Shi, X. Fan, D.C.W. Tsang, F. Wang, Z. Shen, D. Hou, D.S. Alessi, Removal of lead by rice husk biochars produced at different temperatures and implications for their environmental utilizations, *Chemosphere*, 235 (2019) 825-831.
- [5] V. Choudhary, M. Patel, C.U. Pittman, D. Mohan, Batch and Continuous Fixed-Bed Lead Removal Using Himalayan Pine Needle Biochar: Isotherm and Kinetic Studies, *ACS Omega*, 5 (2020) 16366-16378.

[6] S. Cheng, Y. Liu, B. Xing, X. Qin, C. Zhang, H. Xia, Lead and cadmium clean removal from wastewater by sustainable biochar derived from poplar saw dust, Journal of Cleaner Production, 314 (2021) 128074.

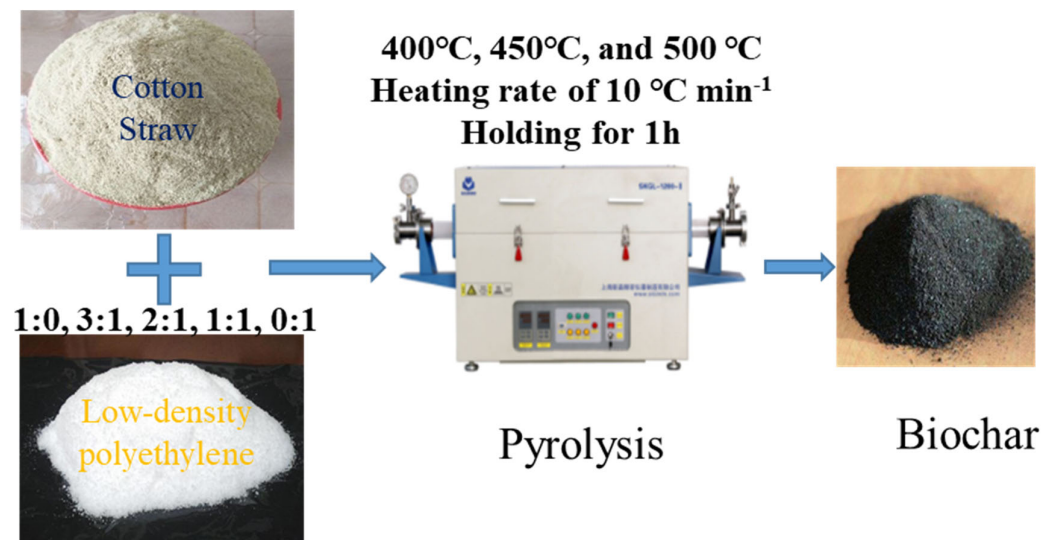


Figure S1. The experimental setup of vertical pyrolysis furnace.